Application of Computational Fluid Dynamics to Investigate Flows Past a Sphere

Leah Gaeta
ME 303: Fluid Mechanics
ltgaeta@bu.edu

April 30, 2020

1 Introduction

In the field of fluid mechanics, often the engineer seeks to understand the flow patterns around objects. Computational Fluid Dynamics, or CFD, software proves to be a useful tool for simulating particular flows to better understand the velocity, pressure, and vorticity fields. The goal of this laboratory exercise was to use COMSOL Multiphysics, a CFD software, to analyze the flow of a Newtonian, incompressible fluid past a sphere using the continuity and Navier-Stokes equations (Eq. 1 and Eq. 2, respectively), as well as compare the results obtained from using COMSOL with theoretical expectations. Within the following equations, $\vec{v}$ is the velocity, p is the pressure, μ is the viscosity, ρ is the density, and $\vec{g}$ is the gravitational acceleration.

$$\vec{\nabla} \cdot \vec{v} = 0 \tag{1}$$

$$-\vec{\nabla} p + \mu \nabla^2 \vec{v} + \rho \vec{g} = \rho \left(\frac{\partial \vec{v}}{\partial t} + \vec{v} \cdot \vec{\nabla} \vec{v} \right) \tag{2}$$

In this experiment, the flow of silicone oil described by Reynold's numbers of 0.001 and 0.01, and the flow of water described by Reynold's numbers of 100 and 1000, were simulated past a sphere of radius 0.01 m. The Reynold's number can be found by applying Eq. 3 below, in which ρ is the density, U is the velocity, a is the radius, and μ is the viscosity. From this equation, one can easily notice that as viscosity is increased, the Reynold's number decreases closer to zero; we characterize this as Creeping Flow, which was the case of both silicone oil simulations. On the other hand, as viscosity decreases, the Reynold's number increases toward infinite values; this is characterized as Potential flow, which was applicable to the study of both water simulations for this experiment.

$$Re = \frac{\rho U 2a}{\mu} \tag{3}$$

For all four simulations, the flows were assumed to be steady with negligible effects from gravity and axisymmetric symmetry over the sphere. As a result, the Continuity and Navier-Stokes equations described by Eq. 1 and Eq. 2 respectively, can be reduced to the following three equations in cylindrical form described by Eq. 4 – 6 below. These assumptions are imperative for finding analytic solutions to these flows past the sphere.

$$\frac{1}{r} \frac{\partial (r v_r)}{\partial r} + \frac{\partial v_z}{\partial z} = 0 \tag{4}$$

$$-\frac{\partial \rho}{\partial r} + \mu \left(\frac{1}{r} \frac{\partial}{\partial r} (r \frac{\partial v_r}{\partial r}) - \frac{v_r}{r^2} + \frac{\partial^2 v_r}{\partial z^2} \right) = \rho \left(v_r \frac{\partial v_r}{\partial r} + v_z \frac{\partial v_r}{\partial z} \right) \tag{5}$$

$$\frac{\partial \rho}{\partial z} + \mu \left(\frac{1}{r} \frac{\partial}{\partial r} (r \frac{\partial v_z}{\partial r}) + \frac{\partial^2 v_z}{\partial z^2} \right) = \rho \left(v_r \frac{\partial v_z}{\partial r} + v_z \frac{\partial v_z}{\partial z} \right) \tag{6}$$

The drag on the sphere was also analyzed for each simulation since the flows caused the sphere to experience such resistance to motion. Drag force D can be calculated from Eq. 7 below, in which p is the

pressure, τ_w is the shear stress, and A is the area. For potential flow, the viscosity is negligible and the last term can be neglected. For the purposes of this experiment, and the drag coefficient C_d was reported for each of the Reynold's numbers simulations and is described by Eq. 8.

$$D = \int dF = \int pcos(\phi)dA + \int \tau_w sin(\phi)dA \tag{7}$$

$$C_d = \frac{D}{\frac{1}{2}\rho U^2 \pi a^2} \tag{8}$$

2 Procedure

Using COMSOL Multiphysics, 2-D axisymmetric simulations were conducted for the flows past a sphere. As previously described, these simulations were run for creeping flow, in which silicone oil with $\mu = 10Pa \cdot s$ and $\rho = 971\frac{kg}{m^3}$ was used, and water with $\mu = 0.001Pa \cdot s$ and $\rho = 1000\frac{kg}{m^3}$ was used to simulate potential flow. First, the geometry needed to be created, then the specified materials and boundary conditions were added. All pressures were recorded as gauge and a sliding wall was used as one of the boundary conditions. Then, in order to obtain the results needed from this analysis, the mesh was generated to subdivide the continuous geometry into discrete elements. Finally, in each simulation, vorticity profiles were obtained, inlet pressures and the varying surface pressures along the sphere were calculated, and the drag forces were found, in order to conduct the analysis described in the following section.

3 Analysis

Figure 1 below shows the vorticity profiles of silicone oil of Reynold's number $Re = 0.001$ and water of $Re = 1000$. Note that vorticity describes the rotation of fluid elements and that a flow is irrotational when the angular velocity is equal to zero. The arrows on the figure describe the velocity fields of each simulation.

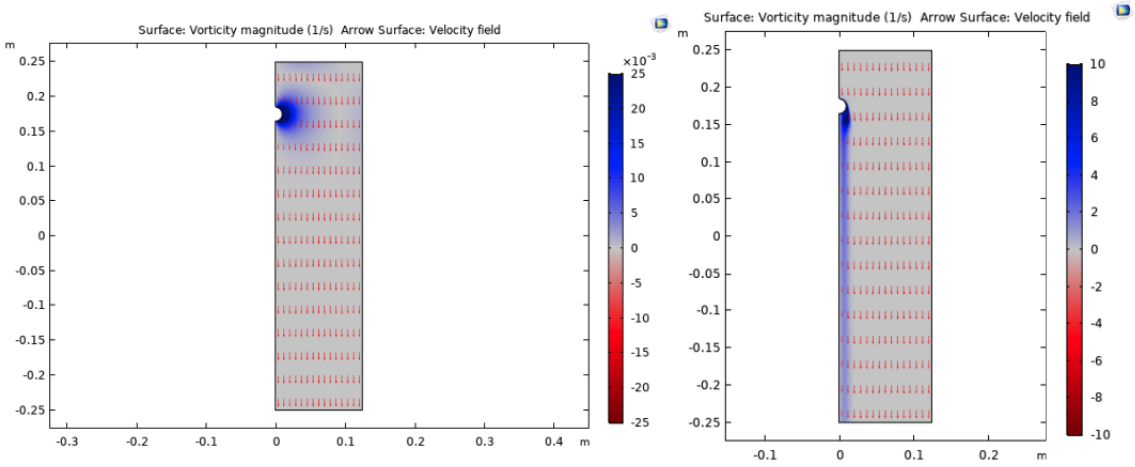

Figure 1: The vorticity profiles for silicone oil $Re = 0.001$ (left) and water $Re = 1000$ (right).

The following two figures describe the change in pressure scaled by the shear stress for silicone and change in pressure scaled by dynamic pressure for water along the sphere for each simulation. The experimental values found are plotted with the theoretical relationships. The pressure scaled by shear stress in creeping flow and the pressure scaled by dynamic pressure for potential flow are described by Eq. 9 and 10 below, respectively.

$$\frac{\Delta p}{\mu U/a} = \frac{3}{2}cos(\phi) \tag{9}$$

$$\frac{\Delta p}{\rho U^2/2} = 1 - \frac{9}{4}sin^2(\phi) \tag{10}$$

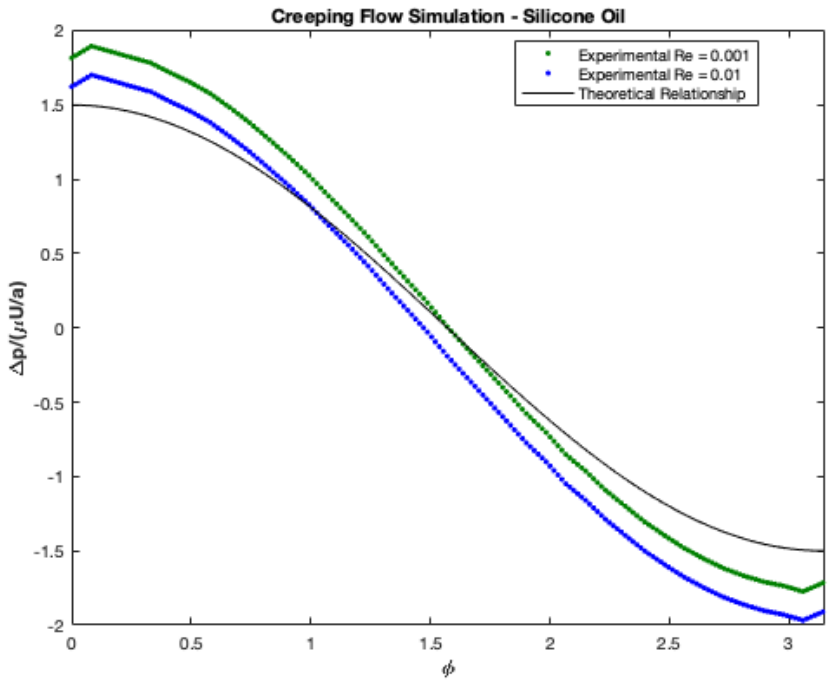

Figure 2: The pressure along the sphere scaled by shear stress for the flow of silicone oil.

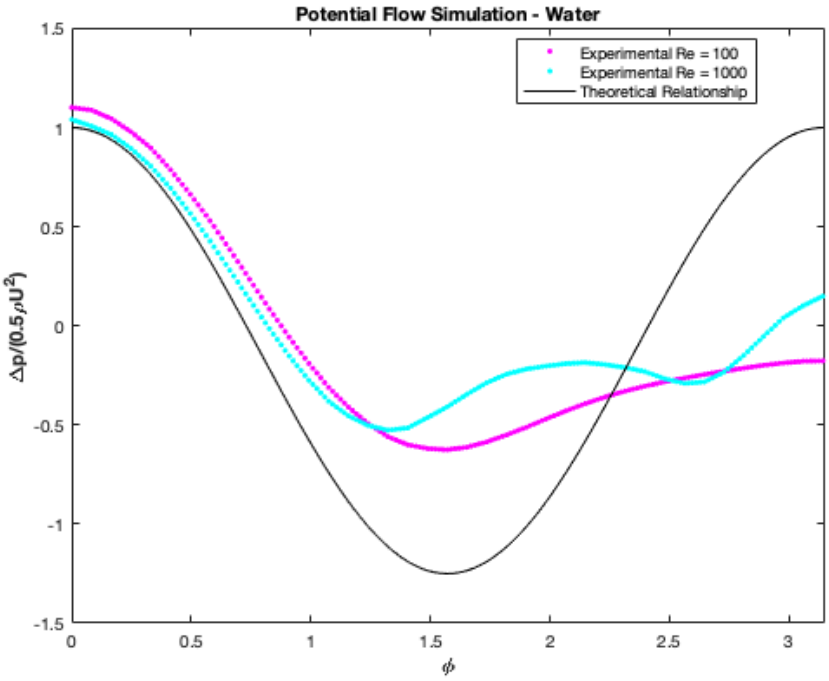

Figure 3: The pressure along the sphere scaled by dynamic pressure for the flow of water.

Finally, Figure 4 describes the relationship between the drag coefficient and Reynold's number on a log-log scale for all four simulations. Note the theoretical relationship of $C_d = \frac{24}{Re}$ and the deviations of the experimentally found values for all four simulations.

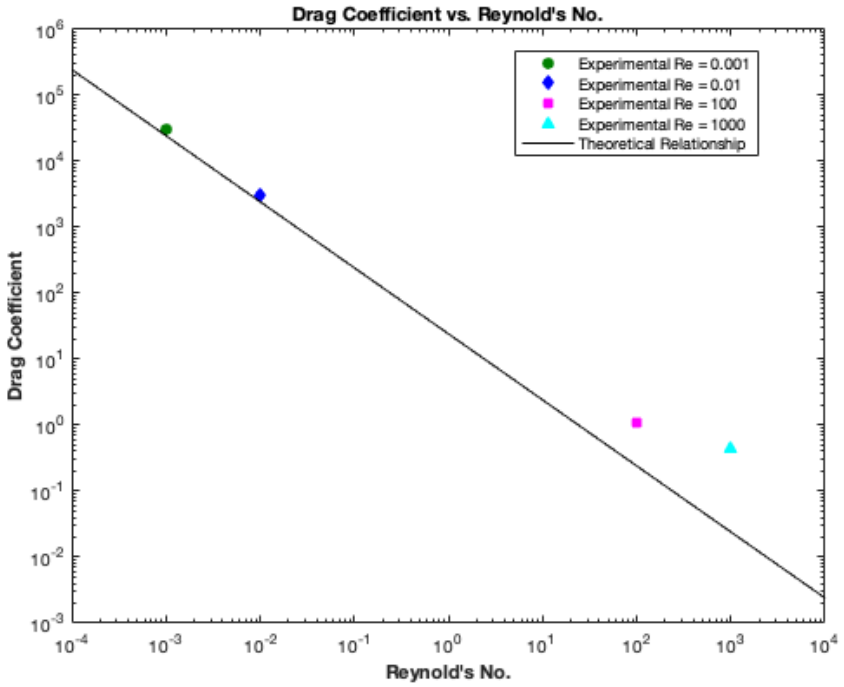

Figure 4: The experimental drag coefficients C_d with respect to their Reynold's numbers and the theoretical relationship.

4 Discussion

Analyzing Figure 1, one will note right away that the vorticity profiles for the silicone oil and water are very different. (Of course, without a sphere there both flows would be uniform and have a vorticity equal to zero.) Though both show vorticity, water has a much higher vorticity magnitude than silicone (as indicated by the scales). In addition, the figure displays that the vorticity is highest along the surface of the sphere for both silicone oil and water, though highest for water. Another point of interest is how once past the sphere, the silicone oil experiences almost no vorticity while the water shows a considerable amount. This suggests that in order to apply Bernoulli's equation, which assumes steady, inviscid, and incompressible flows along a streamline, then Bernoulli's is only valid away from the sphere. For instance, at locations near the wall opposite of the sphere since Bernoulli would apply when the flow is irrotational.

Figure 2 shows that from the simulation, the simulated pressure at the surface of the sphere is very close to the theoretical expectations, suggesting that CFD can be a very powerful tool when modeling creeping flow with small Reynold's numbers around objects. Here it's important to note that silicone oil's density ρ was not important for finding the pressure along the sphere. The small discrepancies that are observed are likely attributed to the assumptions made previously, such as the assumption that there is essentially a Reynold's number equal to zero for creeping flow.

In contrast, Figure 3 shows the water simulations with higher Reynold's numbers of 100 and 1000 and how it varies from the theoretical expected relationship much more. Of interest is how the pressure is very close to what it is expected once the flow hits the sphere but then begins to deviate considerably as approaching the ϕ angle of $\frac{\pi}{2}$ and then deviates further as approaching π on other "side" of the sphere, which coincides with the vorticity profile observed in Figure 1. Therefore, based on the vorticity as well, discrepancies in the potential flow of water should be observed as the theoretical line implies no vorticity. Therefore, if one wanted to create a simulation as close as possible to the theoretical expectations of pressure at the surface, water and other materials with high Reynold's numbers may not be the ones to use. Also worth noting here is that while the density ρ was unimportant for finding the simulated pressure along the sphere for silicone oil, in the case of water it is the viscosity μ that is unimportant, which coincides with Eq. 3 for Reynold's numbers. As the viscosity gets smaller, the Re increases towards infinity while as density gets smaller, the Re decreases towards zero.

Finally, when analyzing the drag force experienced in these four simulations, the numerical data was

relatively consistent with what was theoretically expected. In fact, silicone oil was once again much closer and practically on the theoretical line. Though water does deviate more, the potential flow simulations still showed drag coefficients relatively close to what was expected, which is essentially the aim of using CFD: to make as close approximations of flow as possible. It's important to note though that the theoretical line $C_d = \frac{24}{Re}$ was derived from Stoke's Law (Eq. 7) for creeping flow. Since water represented potential flow here, it should be expected that the silicone oil would not deviate while the water would from the theoretical line representing the relationship between the drag coefficient and the Reynold's number; in fact, water probably should have been simulated with turbulent versus laminar flow conditions as was the case for the silicone oil.

5 Conclusion

The aim of this experiment was to familiarize ourselves with CFD software to aid in the understanding of various Newtonian, incompressible flows past a sphere. This was successfully completed using COMSOL Multiphysics to simulate the creeping flow of silicone oil at Reynold's numbers of 0.001 and 0.01, and the potential flow of water at Reynold's numbers of 100 and 1000. In addition, the drag on the sphere was also found for each of the four simulations. In the cases of studying silicone oil, the results obtained from the software simulations were very close to the theoretical expectations, while those for water varied more. In general though, COMSOL proved to be a very powerful tool for creating such simulations to approximate fluid flow from finite Reynold's numbers, and can therefore be useful for applications beyond the scope of this course.